NONLINEAR DYNAMICS AND CONTROL OF COMPOSITES FOR SMART ENGI DESIGN

An identification of nonlinear dissipative properties of constructional materials at dynamical impact loads conditions

Mirosław Bocian · Krzysztof Jamroziak · Maciej Kulisiewicz

Abstract The dissipative properties of most structural materials are usually described by a viscous damping parameter determining the rate of energy dissipation. The parameter stem from the traditionally adopted rheological Kelvin model. However, the analytical description of the dynamic properties of modern structural materials, including biological materials, often poses difficulties, due to the fact that the stress–strain dependence in these materials is not linear. Therefore a method of determining of nonlinear form of dissipative characteristic $D(x, \dot{x})$ (is presented. As it is assumed, mathematical function of the characteristic consist of nonlinear term $g(x)$ of arbitrary form and so called mixed term $\kappa(x)v$ where $\kappa(x)$ is a function of deformation x and v—velocity of deformation. The deformation of a viscoelastic element which is made of tested material can be measured as displacement x of a single mass m in relative to a point of a complex vibratory system. The proper analysis of the mass m movement allows to evaluate the form of the functions $g(x)$ and $\kappa(x)$ what is a fundamental aim of the presented method. Beside of analytical method description some computer examples are presented. The method can be useful in evaluation of modern structural material properties (e.g. composites).

1 Introduction

The identification of the mechanical properties of materials and structures (e.g. ballistic shields) subjected to impact loads is a major technological and scientific challenge. The difficulties encountered in such identification generally arise from the following causes:

– the behaviour of modern materials used for ballistic shields much differs from the reaction of the traditional linear models based on Hooke's law,
– impact loads are generally random in both their form and frequency of occurrence, i.e. characterized by high unpredictability,
– violently applied loads generate high strain rates, particularly locally in the immediate neighbourhood of the impact,

M. Bocian · M. Kulisiewicz (✉)
The Institute of Materials Science and Applied Mechanics, Wroclaw University of Technology, Smoluchowskiego 25, 50-370 Wrocław, Poland
e-mail: maciej.kulisiewicz@pwr.wroc.pl

M. Bocian
e-mail: miroslaw.bocian@pwr.wroc.pl

K. Jamroziak
Gen. Tadeusz Kosciuszko Military Academy of Land Forces, Czajkowskiego 109, 51-150 Wrocław, Poland
e-mail: krzysztof.jamroziak@wso.wroc.pl
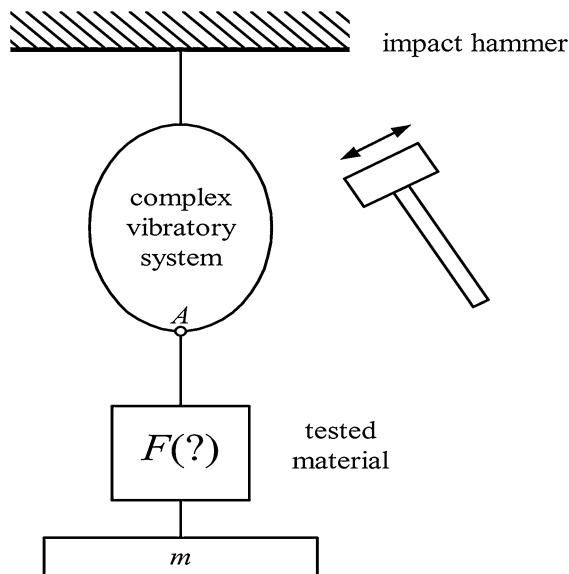
Fig. 1 Schematic of tested system

– under an impact load the temperature of the material rises markedly whereby its mechanical properties may significantly change locally.

The magnitude of the energy dissipation forces produced by internal friction cannot be determined by ordinary quasi-static tension (compression) tests, consisting in determining the dependence between loading force P and strain x for constant (usually very low) rate v_0, since the forces practically do not manifest themselves. In such strength tests the influence of the dissipation forces can be observed only when rates v_0 are high. Relevant test results for both metals and modern lightweight engineering materials based on plastics (laminates, composites, etc.), and also for biological and medical materials, have been reported [1–7]. In order to identify a parameter(s) describing the dissipative properties of materials either rates v_0 in ordinary strength tests should be maximally increased or separate identification methods should be developed for fast-variable dynamic loads, using atypical (generally, nonlinear) mathematical models. Considering that the former approach has a serious practical limitation (in order to increase the strain rate from zero at standstill to the high value of v_0 at which the strength test is carried out great forces need to be applied to produce suitably fast accelerations), the present authors adopted the latter approach. According to the authors' idea, a simple model, in

which a single element made of the tested material with unknown mechanical properties acts on single concentrated mass m (which can move in only one specified direction), is assumed. Such a case occurs, for example, when the tested structural member at one of its ends is fixed to a moving dynamic system while concentrated mass m is fixed to its other (opposite) end, as shown in Fig. 1. This movable system can consist of linear or non-linear dynamic system with any number of degrees of freedom. The necessary condition for the application of the method presented in this paper is that after impact the system should be vibrate, particularly that the point A of this system should vibrate.

In this case, the differential equation of motion of mass m assumes the form:

$$m\ddot{x} + F(?) = -ma_0, \tag{1}$$

where x stands for displacement of mass m relative to point A of the moving system and a_0 is the acceleration of point A. Assuming, similarly as in most papers on dynamic system identification (e.g. [8–14]), that force F of material impact on the mass depends on displacement x and velocity $v = \dot{x}$, the present authors postulate that the force can be described by the following function:

$$F(?) = F(x, \dot{x}) = f_s(x) + D(x, \dot{x}), \tag{2}$$

where component $f_s(x)$ represent any pure elastic interaction and component $D(x, \dot{x})$—dissipative interaction.

It is assumed that function $D(x, \dot{x})$ can be written in the form:

$$D(x, \dot{x}) = g(\dot{x}) + \kappa(x)\dot{x}, \tag{3}$$

where $g(x)$ can be any nonlinear function of velocity while $\kappa(x)$ can be any nonlinear function of displacement x of mass m. Moreover, it is assumed that the following conditions are satisfied:

$$f_s(x = 0) = 0, \quad \kappa(x = 0) = 0. \tag{4}$$

A scheme of such a system is shown in Fig. 2.

The model which has been shown schematically in the Fig. 2 is an extension of the typical linear Kelvin model. In this assumption the influence of the velocity v of the deformation x is described by the function $D(x,v)$ and it is independent of the purely elastic interactions described by the function $f_s(x)$ of any nonlinear form. The adoption of the function $D(x,v)$ in the
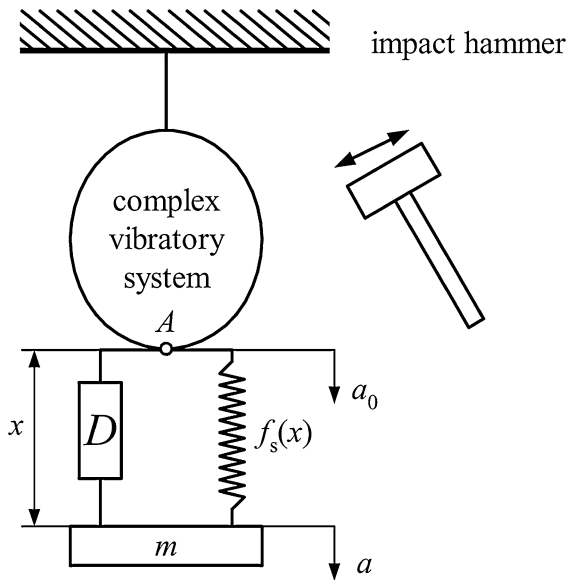
Fig. 2 Schematic of adopted configuration of tested member

form (3) has been motivated by the fact that the damping effect may increase with the increasing deformation of the material. Because of that, the function $\kappa(x)$ has been introduced, which specifies how the damping coefficient changes as the strain level x_0 in the tested structural member increases. Function $\kappa(x)$ defines how the damping coefficient changes as the strain level x_0 in the tested structural member increases.

For example, considerable deformation of a structural member made of a composite material one of the components of which is a liquid (e.g. liquid resin) may cause the constriction and curving of the small channels in which this liquid occurs (see Fig. 3), impeding its flow, which, in turn, may affect the rate of vibration decay.

It is apparent that if $x = 0$, dissipative function $D(x, \dot{x})$ depends solely on the rate in the way described by function $g(\dot{x})$ since $\kappa(x = 0) = 0$ (see conditions 4).

The aim of this paper is to present a method of identifying the dissipative properties of materials if one uses function $D(x, \dot{x})$ in form (3) to describe them. The proposed method consists in determining unknown functions $g(\dot{x})$ and $\kappa(x)$ on the basis of appropriate experimental investigations, assuming that function $f_s(x)$, describing purely elastic properties, is known.

2 Description of method

The differential equation of motion for mass m suspended by means of the tested member from point A of an arbitrarily complex dynamic system has the form

$$ma + F(x, \dot{x}) = 0. \tag{5}$$

If one assumes form (2) of function F in which component $D(x, \dot{x})$ has form (3), Eq. (5) becomes
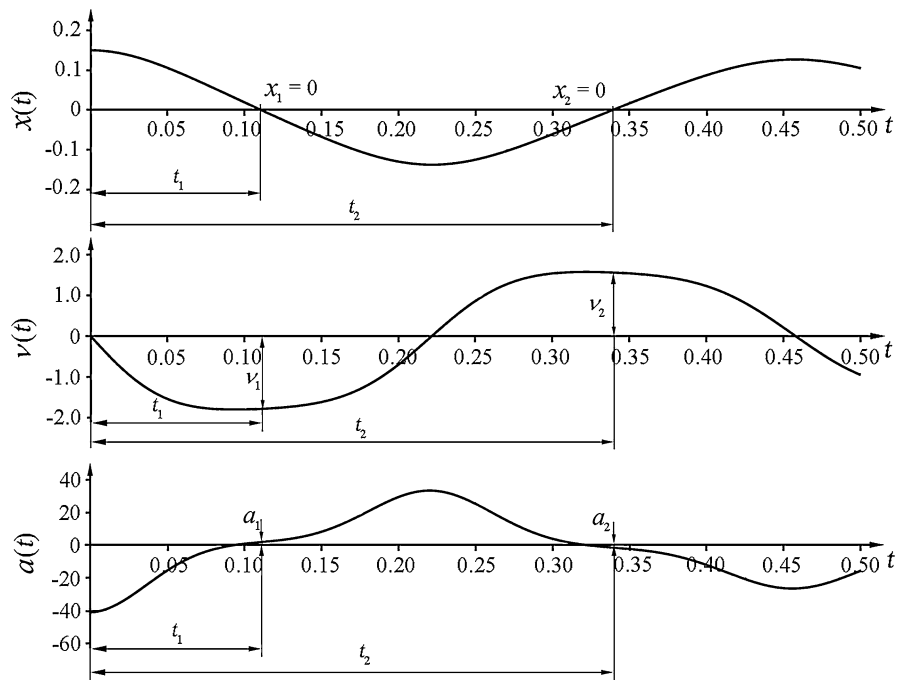
$$ma + g(\dot{x}) + \kappa(x)\dot{x} + f_s(x) = 0, \tag{6}$$

where x—stands for the displacement of mass m relative to point A, v—relative velocity and a—represents its absolute acceleration.
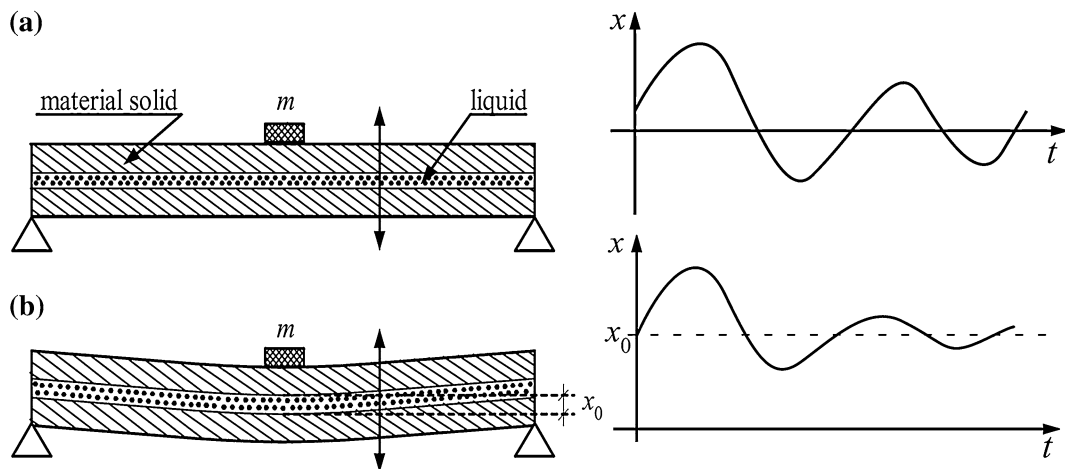
Fig. 3 Effect of material deformation level on free vibration decay rate: **a** system with deformation level $x_0 = 0$, **b** system with deformation level x_0 0 (material solid, liquid)

Fig. 4 Way of determining data a_1, v_1

It should be noted that the Eq. (6) is satisfied for any dynamic excitations applied to the complex vibratory system. This don't have to be impact loads only but also the continuous vibrating forces and forces in any other form (e.g. random ones). Figure 4 presents an exemplary timing diagram which illustrates the vibrations of the mass m in relation to the point A, where: x—represents the relative displacement, v—relative velocity and a is the absolute acceleration of the mass m. In the experiment these quantities can be measured independently but the speed $v(t)$ can be created by integrating the displacement $x(t)$ (e.g. by the numerical method ode45 from the Simulink software).

Assuming that component $f_s(x)$ is known (e.g. it has been determined through simple static tests under constant loads), first function $g(v)$ is determined in the desired range of rates. For this purpose one can select such time instants t_i for which the following is satisfied (see Fig. 4):
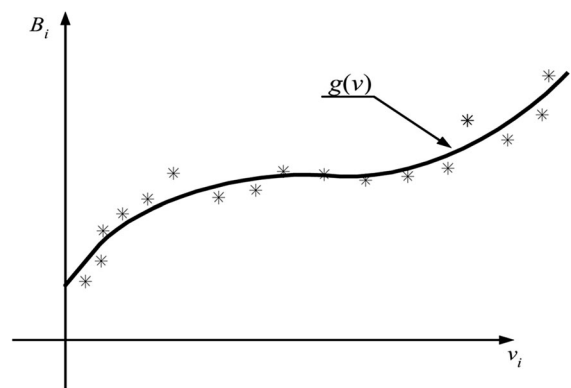
$$x(t_i) = 0, \tag{7}$$

for $t = t_i$, taking into account conditions (4), from Eq. (6) one gets the relation

$$ma_i + g(v_i) = 0, \tag{8}$$

where

$$a_i = a(t = t_i), \quad v_i = v(t = t_i). \tag{9}$$

Fig. 5 Way of determining component $g(v)$ of dissipative characteristic $D(x, \dot{x})$: *points B_i, v_i determined experimentally, function $g(v)$ obtained by approximating relation $B_i(v)_i$
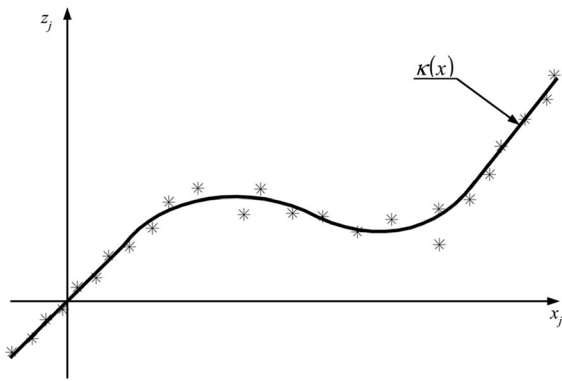
Relation (8) means that in selected instants t_i inertial force B acting on mass m is counterbalanced only by component $g(v)$ of dissipative force D. Hence the following relation is obtained

$$B_i = g(v_i), \tag{10}$$

where

$$B_i = -ma_i. \tag{11}$$

Knowing accelerations a_i and mass m, one can calculate B_i for given values of velocity v_i. Relation

Fig. 6 Way of determining function $\kappa(x)$ of characteristic $D(x, \dot{x})$: * points x_j, z_j determined experimentally, function $\kappa(x)$ obtained by approximating relation $z_j(x_j)$

$B_i(v_i)$ is defined by function $g(v)$. Therefore one can determine function $g(v)$ in a range of experimentally obtained values v_i (see Fig. 5).

Then, already knowing function $g(v)$, one can determine function $\kappa(x)$. For this purpose, one should select such time instants t_j for which acceleration a is equal to zero, i.e.

$$a(t = t_j) = 0. \tag{12}$$

Subsequently, on the basis of Eq. (6), for $t = t_j$ one gets:

$$g(v_j) + \kappa(x_j)v_j = -f_s(x_j), \tag{13}$$

where

$$v_j = v(t = t_j), \quad x_j = x(t - t_j). \tag{14}$$

Hence from relation (13) one gets

$$\kappa(x_j) = \frac{1}{v_j}\left[-f_s(x_j) - g(v_j)\right]. \tag{15}$$

The numerical values z_j on the right side of the above equation, i.e.

$$z_j = \frac{1}{v_j}\left[-f_s(x_j) - g(v_j)\right], \tag{16}$$

can be calculated if the two functions: $f_s(x)$ and $g(v)$ are known. Hence through the approximation of relation $z_j(x_j)$ one can determine function $\kappa(x)$ (see Fig. 6).

However, relation (16) may generate large errors if values v_j are close to zero. For this reason, experimental studies were carried for selected cases, by running simulations.
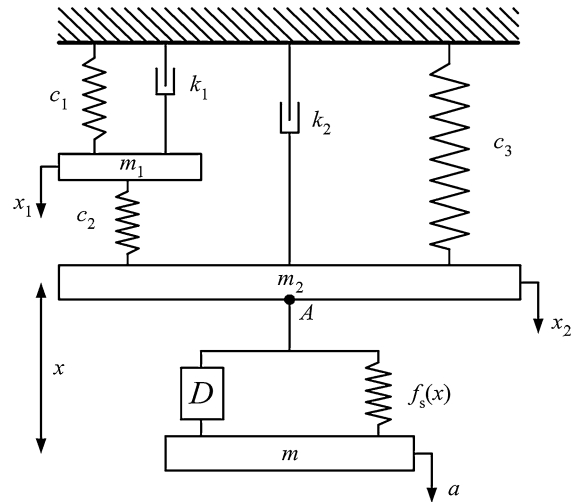
Fig. 7 Schematic of system used in simulation studies

3 Experimental studies

The method was verified, using the computer simulation technique, for a specific dynamic system with three degrees of freedom. A schematic of the system is shown in Fig. 7. The identified system was suspended from a two-mass dynamic system at point A of mass m_2. The whole system consisted of three masses m_1, m_2, m, which could move vertically. Thus the number of degrees of freedom of the whole system amounted to $N = 3$.

The motion of the system was assumed to be described by the following generalized coordinates:

x_1—the displacement of mass m_1 relative to an inertial reference system,

x_2—the displacement of mass m_2 relative to the inertial reference system,

x—the displacement of mass m relative to mass m_2.

For the above generalized coordinates the differential equations of system motion are as follows:

$$m_1\ddot{x}_1 + k_1\dot{x}_1 + c_1x_1 + c_2(x_1 - x_2) = p(t), \tag{17}$$

$$m_2\ddot{x}_2 + k_2\dot{x}_2 + c_3x_2 + c_2(x_2 - x_1) = 0, \tag{18}$$

$$ma + g(v) + \kappa(x)v + f_s(x) = 0, \tag{19}$$

where x, v—relative displacement and relative velocity however a is the acceleration of mass m relative to the inertial reference system, i.e.

$$a = \ddot{x}_2 + \ddot{x}. \tag{20}$$

Table 1 Values of parameters used in simulation numerical

|		
$m_1 = 16$ kg	$m_2 = 40$ kg	$m = 15$ kg
$c_1 = 2000$ N/m	$c_2 = 3500$ N/m	$c_3 = 1700$ N/m
$k_1 = 68$ kg/s	$k_2 = 95$ kg/s	

The studies were carried out for the system with the following numerical values of the constant parameters (Table 1):

Functions $f_s(x)$, $\kappa(x)$ were assumed to be linear and have the following forms:

Fig. 8 Example of pulse load applied to mass m_1
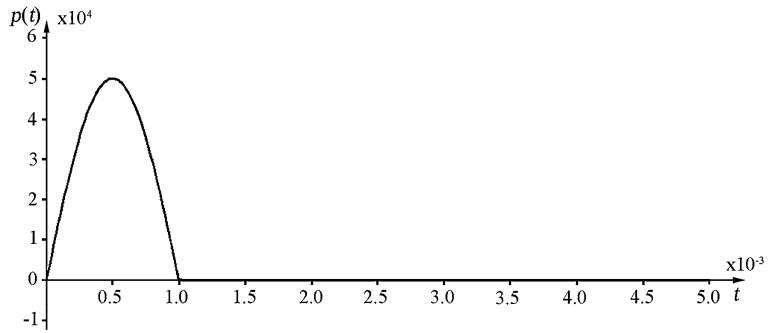
Fig. 9 Sample system responses to pulse loads ($g(v) = 80\mathrm{arctg}(v)$): **a** displacement, **b** velocity, **c** acceleration
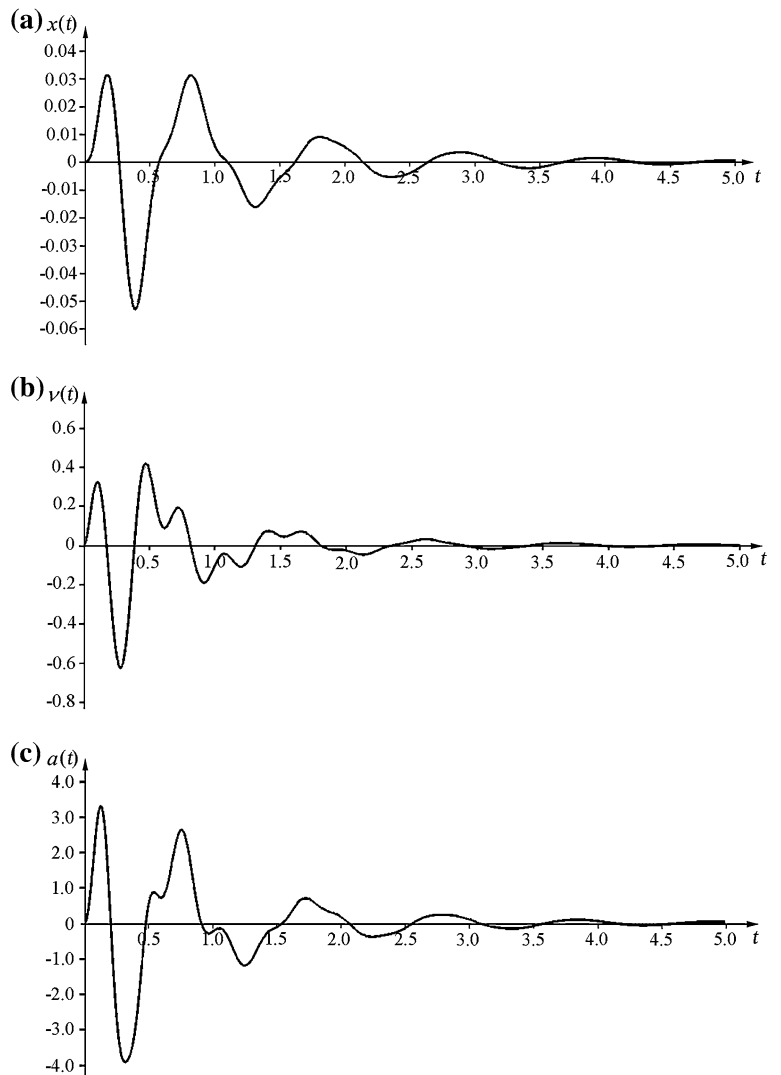
$$f_s(x) = 900x, \tag{21}$$

$$\kappa(x) = 760x. \tag{22}$$

Function $g(v)$ was assumed to have both the linear form
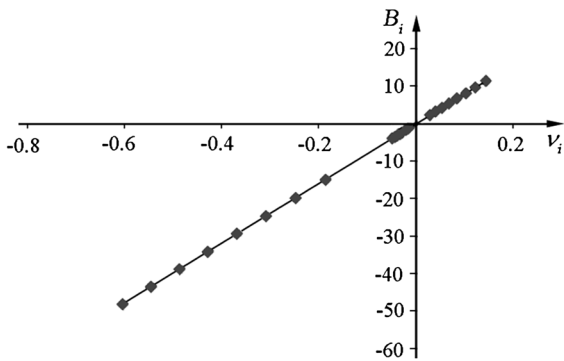
$$g(v) = 80v, \tag{23}$$

and the two following nonlinear forms:
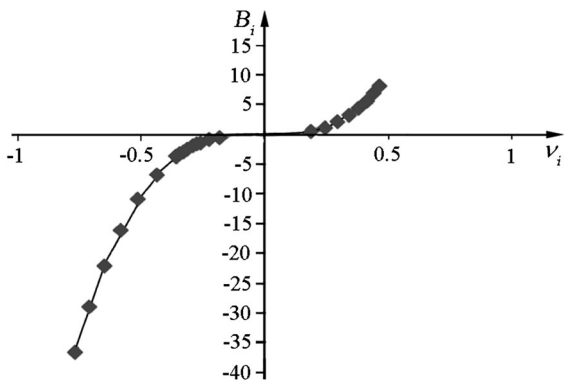
$$g(v) = 80v^3, \tag{24}$$

$$g(v) = 80\mathrm{arctg}(v). \tag{25}$$

The aim of the studies of the modelled system was to experimentally determine the shape of the adopted functions $g(v)$ and $\kappa(x)$. Impact loads in the form of single pulses applied to mass m_1 were used in the experiment. The pulses had a half-sinusoidal shape (see Fig. 8) with a randomly prescribed amplitude.

The duration of each applied pulse was constant and amounted to $T = 0.001$ s. Sample waveforms of system responses x, v, a are shown in Fig. 9.
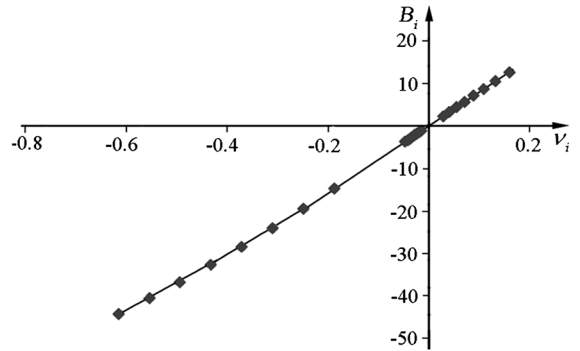
Selecting the values of v_i, a_i from the diagrams, as shown in Sect. 2, dependences $B_i(v_i)$ (see Figs. 10, 11, 12) were obtained and presented as points in the diagrams of assumed functions $g(v)$. As one can see,

Fig. 12 Dependence $B_i(v_i)$ for assumed function $g(v) = 80v\mathrm{arctg}(v)$
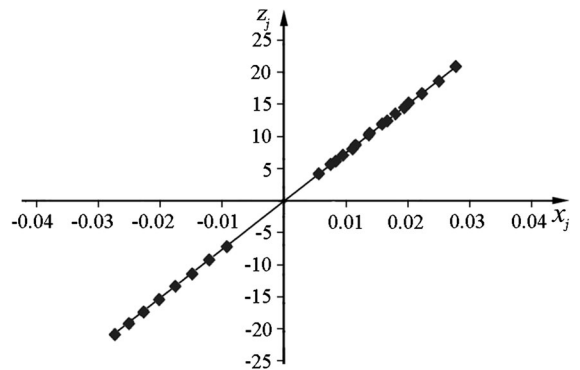
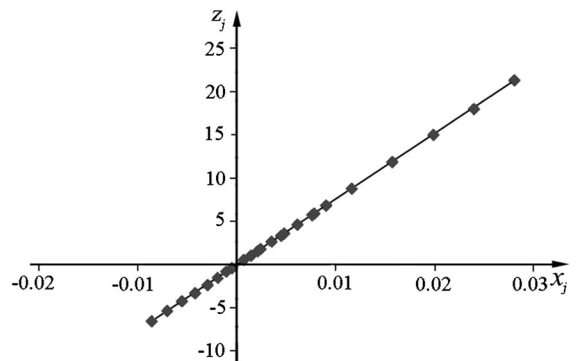**Fig. 13** Dependence $z_j(x_j)$ for assumed function $\kappa(x) = 760x$ and $g(v) = 80v$

Fig. 10 Dependence $B_i(v_i)$ for assumed function $g(v) = 80v$
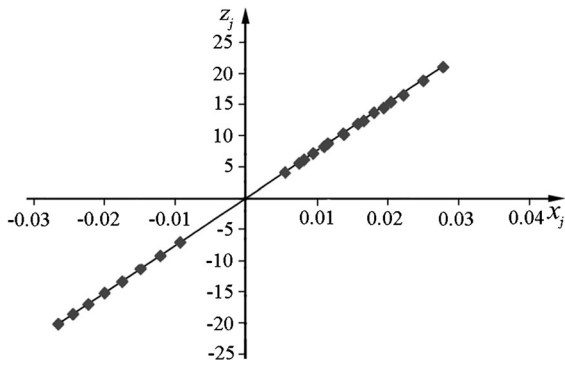

Fig. 11 Dependence $B_i(v_i)$ for assumed function $g(v) = 80v^3$

Fig. 14 Dependence $z_j(x_j)$ for assumed function $\kappa(x) = 760x$ and $g(v) = 80v^3$

**Fig. 15** Dependence $z_j(x_j)$ for assumed function $\kappa(x) = 760x$ and $g(v) = 80v\,\mathrm{arctg}(v)$

the points practically coincide with the graphs of functions $g(v)$ in the forms (23), (24), (25).

Similar results were obtained in the second stage of verification in which function $\kappa(x)$ was determined. In this case, z_j values for the selected values of x_j, v_j were calculated from formula (16). The $z_j(x_j)$ dependence points are shown together with the prescribed linear function $\kappa(x)$ in form (22) in the diagrams below. As one can see, the points ideally coincide with the graph of function $\kappa(x)$ (see Figs. 13, 14, 15).

Additionally this method was used to identify damping pads in the suspension system, which is shown in Fig. 16. These pads was made of a specially
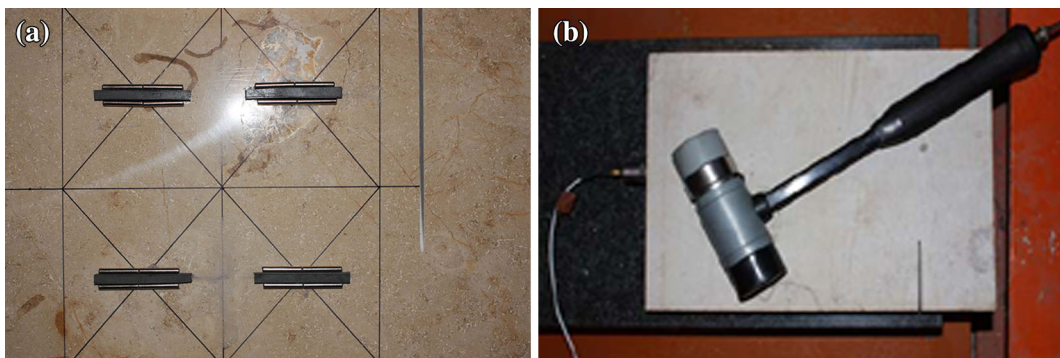
Fig. 16 View of test bed of research: **a** distribution washers, **b** top view of the test object

Fig. 17 Experimental determination component $g(v)$ of dissipative characteristic for tested object

$g(v) = k_1 v - k_3 v^3$

$k_1 = 5.05(\pm 0.2)\cdot 10^3$

$k_3 = 21.8(\pm 3.3)\cdot 10^3$
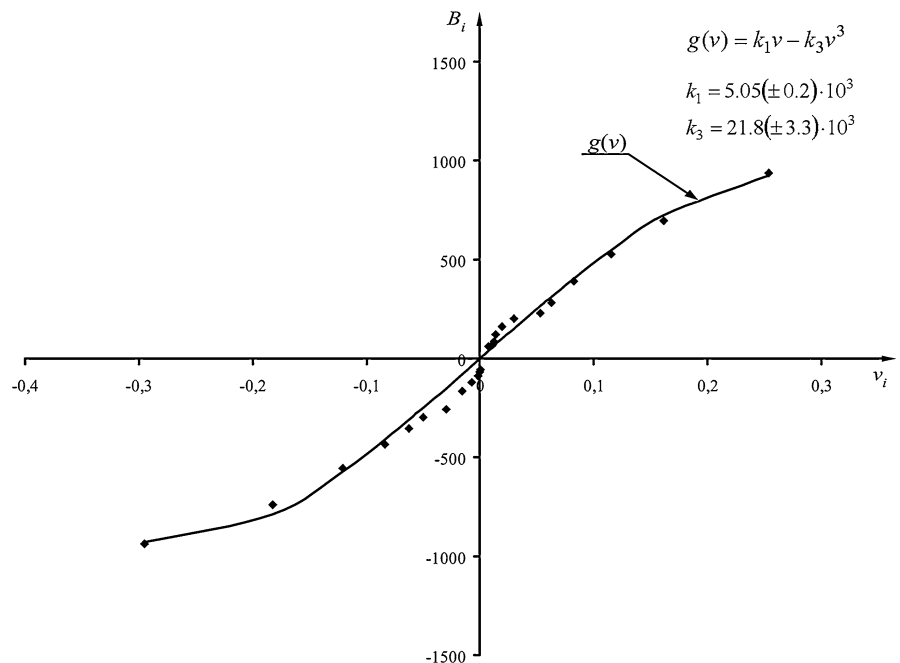
magnetorheological elastomer (their properties can be varied by controlling the intensity of the magnetic field).

This material is produced at the Institute of Materials Science and Applied Mechanics of the Wroclaw Technical University. It is built on the basis of three components: T'efabloc TO222 30A manufactured by CTS Cousin–Tessie (matrix), iron powder ASC300 manufactured by Höganäs AB (ferromagnetic refill) and paraffin oil (supplement which softens the matrix) [15].

Four of such pads supported the horizontal aluminum plate weighing 15 kg (see Fig. 16a). The tested system has been placed on a thick steel plate which hanged by the ropes of the heavy grate that severed as a pedestal for dynamic tests of various light mechanical systems. The whole structure which was very complex, formed a kind of unspecified complex vibratory system. It should be emphasized that the properties and motion type of this system do not influence the results of identification equations of the presented methods. Force carried out in a horizontal

Fig. 18 Experimental determination component $\kappa(x)$ of dissipative characteristic for tested object

$$\kappa(x) = \kappa_0 x^2$$
$$\kappa_0 = 7.7(\pm 0.2)\cdot 10^9$$
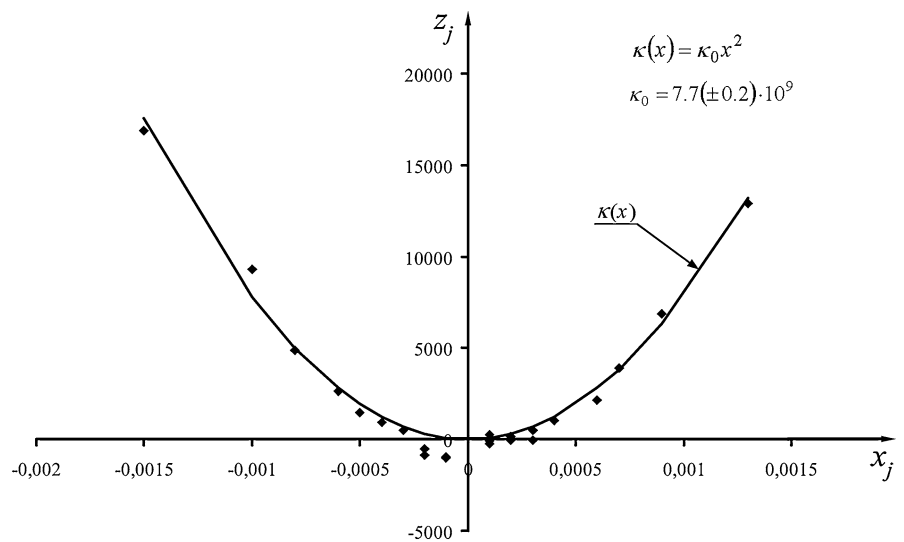
Fig. 19 The examples of the time charts which are necessary to identify the tested system
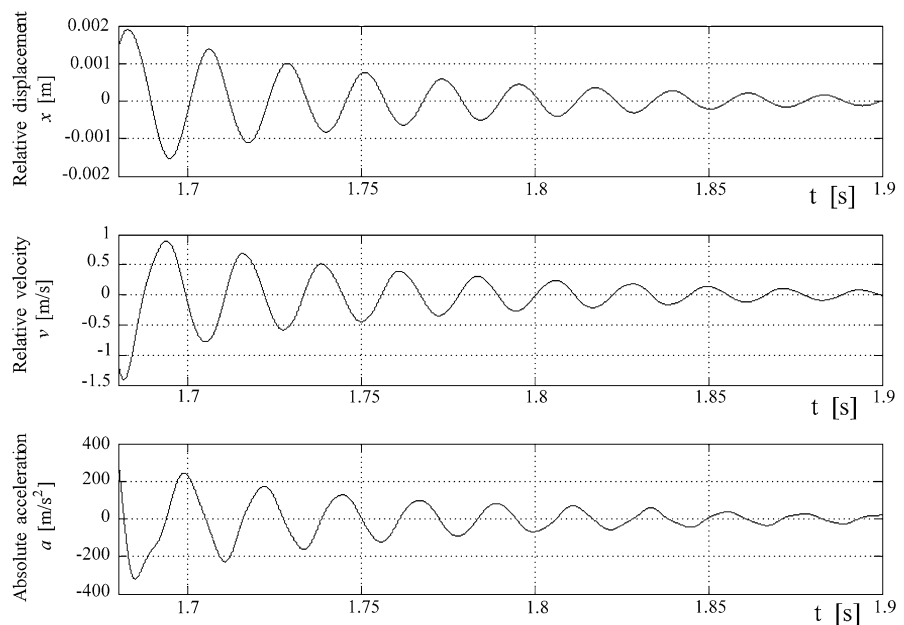
direction with a hammer modal HP. The results for identification of the object type are shown in Figs. 17 and 18. The functions $g(v)$ and $\kappa(x)$ have been obtained by nonlinear regression method application.

The presented results suggests that the dissipative force D has in this case (in such range of velocity and displacement) the form:

$$D = k_1 v + k_3 v^3 + \kappa_0 x^2 v, \qquad (26)$$

where: $k_1 = 5.05 \times 10^3$ Ns/m, $k_3 = -21.8 \times 10^3$ Ns^3/m^3, $\kappa_0 = 7.7 \times 10^9$ Ns/m^3.

Figure 19 presents an example of the recorded time charts of the tested system used to designate the values which are necessary for identification.

4 Conclusions

The presented method of identification was derived from the Eq. (6). The purpose of this method is to determine the shape of the dissipative function $D(x,v)$ in the adopted form (3). The differential Eq. (6) describes the dynamic behavior of the concentrated mass m in relation to the moving system—particularly in relation to the point A. This is a ordinary second-order equation which solution depends on the initial conditions. It may be noted that its solution may also depend on the boundary conditions and the shape effects of the complex vibratory system. It has been included in the component ma because $a = a_A + \ddot{x}$ and a_A is the absolute acceleration of the point A of the complex system which can be both a discrete system and continuous system or even the discrete–continuous system. However, the identification results obtained by this method do not depend on the properties of the complex system (like the weight) as long as the point A of this system has oscillating movement. Although the total mass of the complex vibratory system has a significant influence on the scope and quality of the vibrations of the point A and the entire system it does not affect the results of the identification of the subsystem made of the tested material. If the mass of the complex vibratory system will increase this will require the use of higher excitation forces—vibrations of the point A (and consequently the changes of velocity and relative displacements) should be within the range for identification of the material.

The system shown in the Fig. 7 has been pre-verified based on the presented method. The complex vibratory system was, in this case, the linear dual-mass system while the nonlinear elements include the component D of the tested system. It can be seen that the results of the identification (see Figs. 10, 11, 12, 13, 14, 15) come out almost perfectly. The results obtained for the real system (see Figs. 17, 18 and the function (26)) seem acceptable. It can be noted that the obtained function $g(v)$ presented in the graph (Fig. 17) doesn't describe very accurately the experimental dependence $B_i(v_i)$ in the range near zero and specifically—in the range from $v = -0.04$ to $+0.04$. Presently it is not known whether this is due to the experiment errors or some important feature of the system. Therefore, it seems that the study should be repeated in this range of vibrations.

Summing up, result of the previous research conducted by the authors suggest that:

- the method can be applied to any dynamic excitations including shock loads,
- the method allows to determine the energy dissipation in the process of piercing ballistic in a much more precise than for traditionally used Kelvin dynamical model,
- the computer simulation research has shown that developed method works properly from a theoretical point of view,
- experimental verification of this method on some real dynamic systems should be continued.

Finally it can be add that similar method to discover the dissipative function D in case when point A is motionless have been described in a separate work of authors [16]. In such case the shock load can be applied directly on the mass m. As it can be noticed, in such case the Eq. (6) describes vibrations of the system with one degree of freedom and the measurement of the values of a_i and v_i have to be conducted in a free vibration conditions.

Correct and accurate assessment of the dissipative properties of the materials allow to determine the motion of the complex systems which components are made of such materials. When these properties are significantly non-linear, designing such systems can be made with regard to the evaluation of their stability and the phenomena of bifurcation and chaos [17–25].

References

1. Macky M (2007) The increasing importance of the biomechanics of impact trauma. Sadhana 32:397–408
2. Raymond D, Van EC, Crawford G, Bir C (2009) Tolerance of skull to ballistic tempro-parietal impact. J Biomech 42:2479–2485
3. Baier A, Zolkiewski S (2013) Initial research of epoxy and polyester warp laminates testing on abrasive wear used in car sheathing. Eksploatacja i Niezawodnosc 15(1):37–43
4. Barnes HA, Hutton JF, Walters K (1989) An introduction to rheology. Rheology Series 3. Elsevier, Amsterdam
5. Lenci S (2004) Elastic and damage longitudinal shear behaviour of highly concentrated long fibre composites. Meccanica 39:415–439
6. Sarva SS, Deschanel S, Boyce MC, Chen W (2007) Stress-strain behavior of polyurea and polyurethane from low to high strain rates. Polymer 48:2208–2213
7. Pavlović I, Ćirić I, Djekić P, Nikolić V, Pavlović R, Ćojbašić Ž, Radenković Z (2013) Rheological model optimization using advanced evolutionary computation for the analysis of the influence of recycled rubber on rubber blend dynamical behaviour. Meccanica 48:2467–2477
8. Masri SF, Caughey TK (1979) A nonparametric identification technique for nonlinear dynamic problems. J Appl Mech 46(2):433–447
9. Masri SF, Sassi H (1982) Identification and modeling of nonlinear systems. Nucl Eng Des 72(2):235–270
10. Ibanez P (1975) Identification of dynamic parameters of linear and non-linear structural models from experimental data. Nucl Eng Des 25(1):30–41
11. Rice HJ, Fitzpartick JA (1991) The measurement of non-linear damping in single-degree-of-freedom systems. J Vib Acoust 113(1):132–140
12. Jang TS, Choi HS, Han SL (2009) A new method for detecting non-linear damping and restoring forces in non-linear oscillation systems from transient data. Int J Non-Linear Mech 44(7):801–808
13. Roberts JB, Dunne JF, Debonos A (1995) A spectral method for estimation of non-linear system parameters from measured response. J Probab Eng Mech 10(4):199–207
14. Kulisiewicz M (2005) Modeling and identification of nonlinear mechanical systems under dynamic complex loads. University of Technology, Wroclaw
15. Kaleta J (2013) Magnetic materials. Construction, manufacture, study of the properties, application. University of Technology, Wroclaw
16. Bocian M, Kulisiewicz M (2013) Method of identifying nonlinear characteristic of energy dissipation in dynamic systems with one degree of freedom. Arch Civil Mech Eng. doi:10.1016/j.acme.2013.11.006
17. Bocian M, Jamroziak K, Kulisiewicz M (2009) Determination of the chain-like non-linear multi-degree-of-freedom systems constant parameters under dynamical complex loads. PAMM 9(1):397–398. doi:10.1002/pamm.200910172
18. Yao M, Zhang W (2014) Multi-pulse chaotic motions of high-dimension nonlinear system for a laminated composite piezoelectric rectangular plate. Meccanica 49:365–392
19. Awrejcewicz J (1995) Bifurcation and chaos. Springer–Verlag, Berlin
20. Ichiro A (2013) Multiple duffing problem in a folding structure with hill-top bifurcation. Chaos Solitons Fractals 51:52–63. doi:10.1016/j.chaos.2013.02.012
21. Sorokin SV, Tcherniak DM (1996) Nonlinear dynamics and chaos of a finite-degree-of-freedom model of a buckled rod. Meccanica 31:273–291
22. Rega G, Lenci S, Thompson JMT (2010) Controlling chaos: the OGY method, its use in mechanics, and an alternative unified framework for control of non-regular dynamics. In: Thiel M et al. (eds.) Nonlinear dynamics and chaos: advances and perspectives. Springer, Berlin. doi:10.1007/978-3-642-04629-2_11
23. Buchacz A, Galeziowski D (2012) Synthesis as a designing of mechatronic vibrating mixed systems. J VibroEng 14:553–559
24. Warminski J (2010) Nonlinear normal modes of a self-excited system driven by parametric and external excitations. Nonlinear Dyn. doi:10.1007/s11071-010-9679-5
25. Zolkiewski S (2011) Damped vibrations problem of beams fixed on the rotational disk. Int J Bifurc Chaos 21(10):3033–3042. doi:10.1142/S0218127411030337